Stem Cell Reports
Article

OPEN ACCESS

Immune Regulator MCPIP1 Modulates TET Expression during Early Neocortical Development

Huihui Jiang,[1,3] Xiaohui Lv,[1,3] Xuepei Lei,[1,3] Ying Yang,[2] Xin Yang,[2] and Jianwei Jiao[1,*]
[1]State Key Laboratory of Stem Cells and Reproductive Biology, Institute of Zoology
[2]Key Laboratory of Genomics and Precision Medicine, Beijing Institute of Genomics
Chinese Academy of Sciences, Beijing 100101, China
[3]Co-first author
*Correspondence: jwjiao@ioz.ac.cn
http://dx.doi.org/10.1016/j.stemcr.2016.07.011

SUMMARY

MCPIP1 is a recently identified immune regulator that plays critical roles in preventing immune disorders, and is also present in the brain. Currently an unresolved question remains as to how MCPIP1 performs its non-immune functions in normal brain development. Here, we report that MCPIP1 is abundant in neural progenitor cells (NPCs) and newborn neurons during the early stages of neurogenesis. The suppression of MCPIP1 expression impairs normal neuronal differentiation, cell-cycle exit, and concomitant NPC proliferation. MCPIP1 is important for maintenance of the NPC pool. Notably, we demonstrate that MCPIP1 reduces TET (TET1/TET2/TET3) levels and then decreases 5-hydroxymethylcytosine levels. Furthermore, the MCPIP1 interaction with TETs is involved in neurogenesis and in establishing the proper number of NPCs in vivo. Collectively, our findings not only demonstrate that MCPIP1 plays an important role in early cortical neurogenesis but also reveal an unexpected link between neocortical development, immune regulators, and epigenetic modification.

INTRODUCTION

The cerebral cortex is the center of the mammalian brain and provides the structural basis for complex perceptual and cognitive functions. The formation of the cortex relies on the expansion of neural progenitor cells (NPCs) and the subsequent generation of postmitotic neurons. Recent studies have shed light on neurogenesis, the process that underlies expansion of the neocortex whereby NPCs generate neurons. It has been reported that numerous immune proteins are expressed in neural stem cells, suggesting that immune signaling could be involved in the process of neurogenesis (Carpentier and Palmer, 2009). For a better understanding of this new role of immune proteins in brain development and function, it is first necessary to have a basic understanding of their known functions.

Due to the existence of the blood-brain barrier and the immunosuppressive microenvironment, the CNS has been traditionally considered an immune-privileged organ (Sallusto et al., 2012). It has been reported that immune proteins classically thought to have specific immune function such as cytokines, major histocompatibility complex class I molecules, and T cell receptor subunits, are also expressed in the regions of the CNS (Boulanger, 2009; Komal et al., 2014; Syken and Shatz, 2003). Immune molecules play essential roles in various aspects throughout neural development of the CNS (Bauer et al., 2007; Boulanger, 2009). However, the expression, function, and mechanisms of action for the large majority of immune molecules in normal brain development have not yet been studied.

Monocyte chemoattractant protein (MCP)-1-induced protein 1 (MCPIP1) is a recently identified protein harboring a CCCH-type zinc-finger domain (Liang et al., 2008; Xu et al., 2012). It is encoded by the ZC3H12A (zinc-finger CCCH-type containing 12A) gene, which is expressed in interleukin-1β (IL-1β)-induced human monocyte-derived macrophages and MCP-1-stimulated human peripheral blood monocytes (Skalniak et al., 2009; Zhou et al., 2006). MCPIP1 is necessary to inhibit unwanted immune reactions mediated by T cells through destabilizing a set of mRNAs (Uehata et al., 2013). Its deficiency leads to a complex phenotype involving severe anemia, severe inflammatory response, autoimmune response, and premature death (Liang et al., 2010; Matsushita et al., 2009). Structural studies of MCPIP1 reveal that the N-terminal conserved domain shows a PilT N-terminus-like RNase structure, providing further evidence that MCPIP1 has RNase activity. Recently, several studies have focused on the RNase activity of MCPIP1, which targets the mRNAs for IL-6, IL-1β (Matsushita et al., 2009; Mizgalska et al., 2009), and pre-microRNAs (Suzuki et al., 2011). The functional diversity and the RNase structure of MCPIP1 make it an attractive candidate as an immune regulator that mediates normal brain development.

The neurodevelopmental process is orchestrated by a series of intrinsic mechanisms and extrinsic cues. Among these, intrinsic epigenetic regulation plays an important role in neural progenitor fate specification and provides one explanation about the complexity of developmental processes. DNA methylation in the form of 5-methylcytosine (5mC) is essential for normal development in

mammals and influences a variety of biological processes, including transcriptional regulation, imprinting, and the maintenance of genomic stability. Hydroxymethylcytosine is emerging as the active demethylation modification that targets a specific 5-methyl group on cytosine for net removal by a complex base excision repair mechanism (Guo et al., 2011a, 2011b). Consistent with the idea that hydroxymethylcytosine is involved as a specific mechanism for active cytosine demethylation, recent studies identified the ten-eleven translocation (TET) family of proteins in active DNA demethylation (Ito et al., 2010; Tahiliani et al., 2009). The three mammalian TET proteins, TET1, TET2, and TET3, have changed our understanding of the process of DNA demethylation as they can oxidize 5mC to 5-hydroxymethylcytosine (5hmC), 5-formylcytosine (5fC), and 5-carboxylcytosine (5caC) (He et al., 2011; Ito et al., 2010; Tahiliani et al., 2009). Recent studies have shown that TET-mediated DNA demethylation can play vital roles in various biological processes, not only in development but also in disease. Despite these advances, the functions of TET proteins and their regulation in brain development need further investigation.

Here, we report the unique roles of MCPIP1 during early neocortical development. We found a dramatic expression pattern of MCPIP1 during early cortical neurogenesis. MCPIP1 regulates various aspects of neurogenesis. Notably, we observed that MCPIP1 directly targets *Tet*s, and represses TET and 5hmC expression levels. Importantly, the interaction of MCPIP1 and TETs is involved in neurogenesis and NPC pool maintenance. Our current data demonstrate a direct and important molecular link between the immune regulatory molecule, TETs, and epigenetic regulation.

RESULTS

Expression of MCPIP1 in the Developing Neocortex

To elucidate the role of MCPIP1 in early neocortical development, we identified the expression of MCPIP1 in the embryonic cortex. We performed immunostaining experiments in vivo and in vitro to confirm the expression of MCPIP1. The results showed that MCPIP1 was expressed at high levels in the cortical plate (CP), subventricular zone (SVZ), and ventricular zone (VZ) in the developing neocortex, but expressed at low levels in the intermediate zone (Figure 1A). Notably, we found that the expression of MCPIP1 decreased significantly in the VZ but increased significantly in CP from embryonic day 12 (E12) to E18, the main phase of cortical neurogenesis in the mouse developing brain (Figure 1A). These data suggested that MCPIP1 may be expressed in NPCs and neurons. To determine this possibility, we immunostained E12 brain sections and found that MCPIP1 was preferentially expressed in SOX2- and PAX6-expressing NPCs, whereas it was also expressed in TBR2-positive progenitors (Figures 1B–1D). We further determined that MCPIP1 was also strongly expressed in newborn neurons of the CP, as identified by CTIP2 and β-III-tubulin (TUJ1) staining (Figures 1E and 1F). To further confirm these results, we isolated NPCs from E12 mouse brains and analyzed MCPIP1 expression in vitro. The double immunostaining results revealed that MCPIP1 was expressed at high levels in cultured NPCs and newborn neurons (Figures S1A–S1E). Taken together, these data indicate that MCPIP1 is abundantly expressed in NPCs and newborn neurons during the early stages of neurogenesis.

NPCs are multipotent cells characterized by their capability to self-renew and differentiate into multiple cells. Our study showed that at the beginning of neurogenesis MCPIP1 was largely expressed in the expanding cell population of the VZ, which maintains the appropriate pool of neural progenitors and subsequently establishes a functional neocortex. Therefore, we focused our studies on the potential roles of MCPIP1 in early cortical neurogenesis.

MCPIP1 Regulates Neurogenesis in the Developing Neocortex

To determine the potential roles of MCPIP1 in NPCs, we performed gain- and loss-of-function studies to elucidate its function in vivo and in vitro. Two different small hairpin RNAs (shRNAs) to silence *Mcpip1* expression and a DNA plasmid encoding *Mcpip1* were constructed and used for in utero electroporation. All constructs expressed GFP as an indicator. Western blotting results demonstrated that the two shRNAs were capable of reducing MCPIP1 protein levels (Figures S2A–S2D), and the *Mcpip1* expression plasmid could effectively increase MCPIP1 protein expression (Figures S2E and S2F).

Next, we examined the effects of *Mcpip1* knockdown or overexpression in the VZ/SVZ of the mouse cortex using in utero electroporation (Lv et al., 2014a). We electroporated E13 mouse embryonic brains with *Mcpip1* shRNAs or *Mcpip1* expression plasmid, and harvested the electroporated brains 3 days later at E16. We observed a significantly altered distribution of GFP-positive cells in the developing neocortex following *Mcpip1* expression changes. *Mcpip1* knockdown led to an obvious increase in the proportion of GFP-positive cells in the VZ and SVZ with a concomitant decrease in the proportion of GFP-positive cells in the CP. In contrast, *Mcpip1* overexpression resulted in a distribution of GFP-positive cells in the three cortex zones (Figures 2A and 2B). The phenotypes resulting from treatment with the two different shRNAs were identical (Figures S2G and S2H). Together, these results demonstrate that MCPIP1

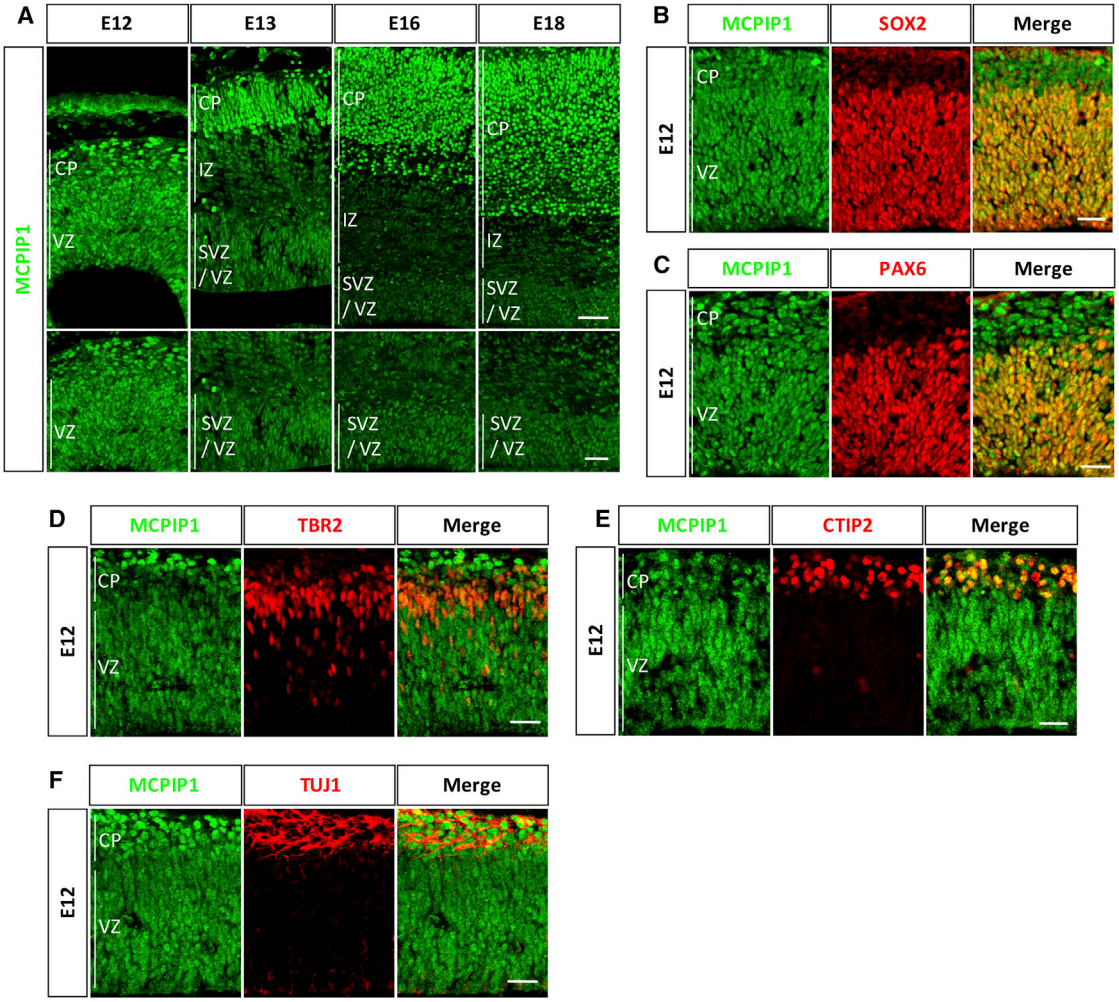

Figure 1. Expression of MCPIP1 in the Developing Neocortex

(A) Immunostaining for MCPIP1 in mouse developing cortex. Embryonic brain sections were immunostained with anti-MCPIP1 antibody. Note that MCPIP1 expression decreased gradually in the VZ from E12 to E18. CP, cortical plate; IZ, intermediate zone; SVZ, subventricular zone; VZ, ventricular zone. Lower panels show enlarged views of ventricular zones. Scale bars, 50 μm (upper) and 20 μm (lower).

(B–D) MCPIP1 is abundantly expressed in early neural progenitors in embryonic cortex. The E12 brain sections were immunostained with anti-SOX2, anti-PAX6, or anti-TBR2 and anti-MCPIP1 antibodies. Scale bars, 20 μm.

(E and F) MCPIP1 is also strongly expressed in newborn neurons in embryonic cortex. E12 brain sections were immunostained with anti-CTIP2 or anti-TUJ1 and anti-MCPIP1 antibodies. Scale bars, 20 μm.

See also Figure S1.

regulates cell distribution during early neocortical development. To exclude apoptosis as a potential cause for the observed phenotypes, we performed TUNEL staining at E15 and E16 brain sections, but did not observe significant differences following *Mcpip1* alteration (Figures S3A–S3D). Meanwhile, we performed immunostaining experiments using cleaved caspase-3 antibody in vitro. The results also showed no obvious differences after *Mcpip1* expression alteration (Figure S3E).

The fact that different proportions of GFP-positive cells remained in the CP following *Mcpip1* expression alteration suggested possible changes in neuronal differentiation. To determine whether MCPIP1 had an effect on neuronal differentiation, we next examined the overlap of the GFP-positive cell population with TUJ1 and MAP2, markers of differentiated neurons, on E16 electroporated brain sections. We found that *Mcpip1* knockdown significantly decreased the levels of TUJ1 and MAP2 compared with controls (Figures 2C–2F). To further confirm the effects of MCPIP1 on neuronal differentiation, we performed in vitro experiments. Primary NPCs isolated from E12 mouse embryonic brains were infected with control,

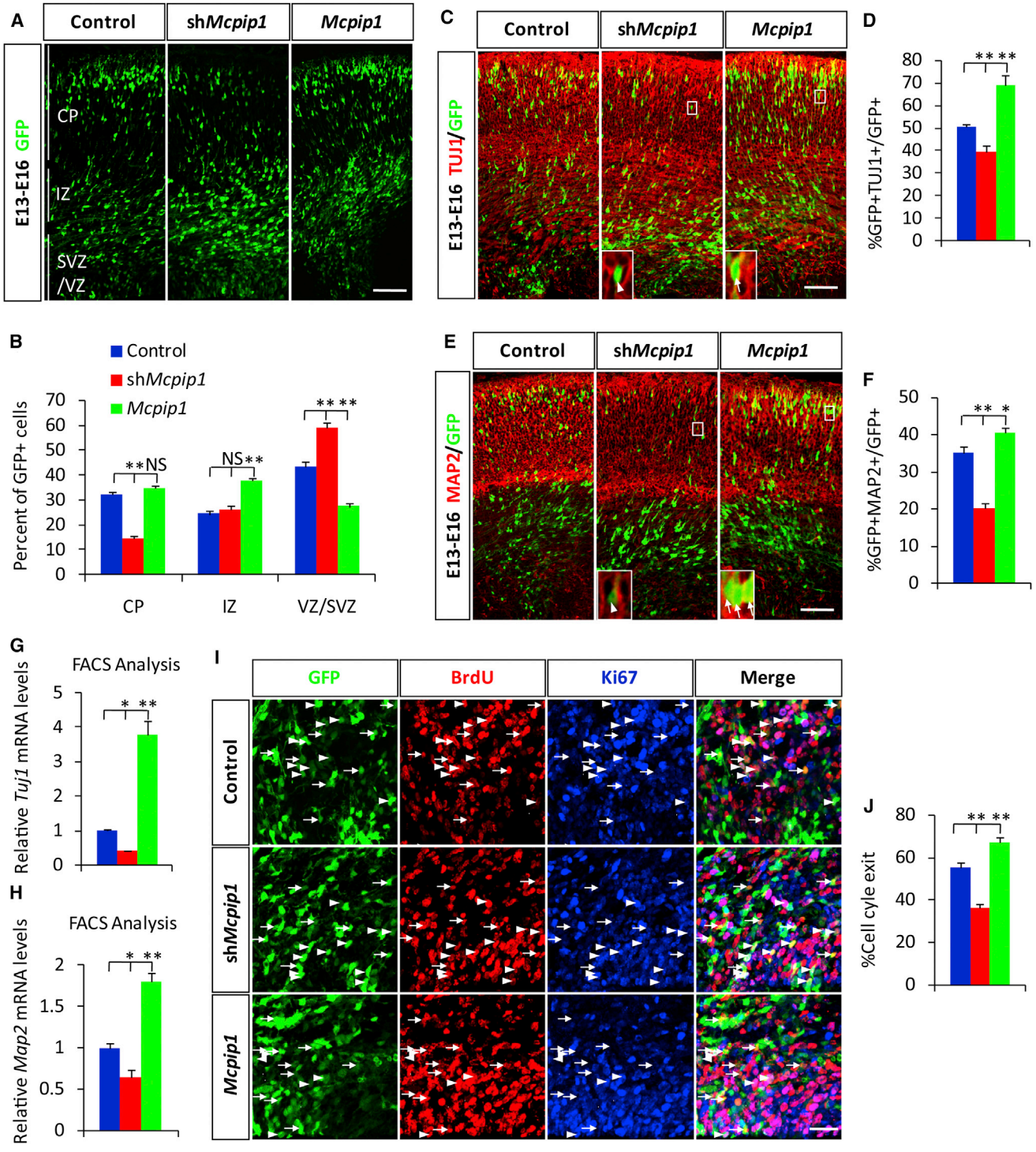

Figure 2. MCPIP1 Regulates Neurogenesis in the Developing Neocortex

(A and B) *Mcpip1* expression variation resulted in altered cell distribution in the cortex. (A) Control, *Mcpip1* shRNA, or *Mcpip1* expression plasmid was electroporated into embryonic brains at E13. The brains were then harvested at E16. Scale bar, 50 μm. (B) The percentage of GFP cells in each region was quantified. Values are presented as mean ± SD; n = 3 independent experiments. **p < 0.01, one-way ANOVA with Tukey's test for post hoc multiple comparisons; NS, not significant.

(C–H) MCPIP1 regulates cortical neuronal differentiation. (C and E) The electroporated E16 brain sections were immunostained with anti-TUJ1 or anti-MAP2 antibody. Inset shows zoom view of colocalization cells in brain sections with *Mcpip1* knockdown or overexpression.

(legend continued on next page)

Mcpip1 knockdown, or *Mcpip1* overexpression lentivirus. After culture in differentiation medium for 3 days, cells were harvested and fluorescence-activated cell sorting (FACS) analysis was performed to ensure the extent of *Mcpip1* overexpression or knockdown (Figures S2I and S2J). Then *Tuj1* and *Map2* mRNA levels were examined by real-time qRT-PCR. The results further confirmed that *Mcpip1* expression variation resulted in significant changes of *Tuj1* and *Map2* expression (Figures 2G and 2H). In addition, the infected NPCs were also examined by immunostaining (Figures S4A and S4B) and western blot (Figures S4C–S4E) with TUJ1 antibody after culture in differentiation medium for 3 days. These results in vitro are consistent with those in vivo. Collectively, these results in vivo and in vitro indicate that MCPIP1 promotes premature neuronal differentiation. Premature neuronal differentiation is closely associated with early cell-cycle exit. To test this possibility, we analyzed the cell-cycle exit index. The embryonic brains were electroporated at E13 and harvested at E16. Bromodeoxyuridine (BrdU) (100 mg/kg) was injected into mice 48 hr after electroporation. The results demonstrated that *Mcpip1* knockdown obviously decreased the cell-cycle exit index (Figures 2I and 2J).

The generation of the proper number of neurons in the developing neocortex depends on a carefully regulated spatial and temporal balance between differentiation and proliferation. Because *Mcpip1* knockdown resulted in defects in neuronal differentiation, we asked whether these defects coincided with changes in NPC proliferation. To investigate this possibility, we performed the NPC culture experiments in vitro. The results showed increased cell proliferation activity following *Mcpip1* inhibition, which were identified by ethynyldeoxyuridine (a proliferation marker also labeling S-phase dividing cells) and Ki67 (a proliferation marker that labels cells in all active phases of the cell cycle) (Figures S4F–S4I). Furthermore, the embryonic brains were electroporated at E13 and BrdU was injected to label S-phase dividing cells 2 hr before euthanasia at E16. The immunostaining results showed that BrdU labeling in the GFP-positive population significantly increased after *Mcpip1* knockdown (Figures S4J and S4L), indicating an overall increase in cell proliferation. Meanwhile, the E16 electroporated brains were also stained with the mitotic marker phosphohistone H3 (pH3), and the results demonstrated a significant increase in mitotic activity (Figures S4K and S4M). Conversely, *Mcpip1* overexpression resulted in a significant decrease in cell proliferation and mitotic index. Taken together, these findings demonstrate that *Mcpip1* knockdown disrupts normal neuronal differentiation, cell-cycle exit, and concomitant NPC proliferation.

MCPIP1 Regulates the Composition of the NPC Pool and Transition of NPCs

Orderly cortical development requires appropriate numbers and types of cells to be derived from the progenitor pools. Two main types of neurogenic progenitor cells are present in the developing cerebral cortex, apical progenitors, and basal progenitors. Apical progenitors, which are capable of self-renewal, are in charge of the maintenance of the progenitor pool during neurogenesis. Basal progenitors, also known as intermediate neural progenitors, are capable of generating the majority of neurons for all layers. The changed neuronal differentiation, cell-cycle exit index, and cell proliferation due to *Mcpip1* expression variation suggested that MCPIP1 may play an important role in regulating the makeup of the neural progenitor pool. To investigate this possibility, we analyzed the electroporated brains at E16 to examine the makeup of the progenitor pool by immunohistochemistry for PAX6, the apical progenitor marker, and TBR2, the basal progenitor marker. These results indicated that MCPIP1 decreased the number of apical progenitors and increased the number of basal progenitors (Figures 3A–3D). Meanwhile, in vitro FACS and subsequent qRT-PCR analysis further confirmed that *Mcpip1* expression variation caused correlated changes of *Pax6* and *Tbr2* mRNA expression levels (Figures 3E and 3F). Taken together, these findings reveal that MCPIP1 is critical for the maintenance of the NPC pool.

Comparatively, apical progenitors are often considered as the predominant progenitor due to their ability to

Arrows indicate GFP-TUJ1 or GFP-MAP2 double-positive cells; arrowheads indicate GFP^+ $TUJ1^-$ or GFP^+ $MAP2^-$ cells. (D and F) The quantitative percentage of GFP-TUJ1 or GFP-MAP2 double-positive cells is displayed. (G and H) Meanwhile, E12 primary NPCs were infected with *Mcpip1*-expressing or *Mcpip1* shRNA-expressing lentivirus, and harvested for FACS analysis after culture for 3 days. Then, qRT-PCR analysis was performed to examine *Tuj1* and *Map2* mRNA levels. Values are presented as mean ± SD; n = 3 independent experiments. *p < 0.05; **p < 0.01, one-way ANOVA with Tukey's test for post hoc multiple comparisons. Scale bars, 50 μm.

(I and J) MCPIP1 regulates the cell-cycle exit index. (I) Embryonic brains were electroporated at E13. BrdU (100 mg/kg) was injected into mice 48 hr after electroporation, and brains were harvested at E16. The brain sections were immunostained for BrdU and Ki67. Arrows indicate GFP^+ $BrdU^+$ $Ki67^-$ cells. Arrowheads indicate GFP^+ $BrdU^+$ $Ki67^+$ cells. Scale bar, 20 μm. (J) Quantification of cell-cycle exit index (the percentage of the GFP^+ $BrdU^+$ $Ki67^-$ cells relative to the GFP^+ $BrdU^+$ cells) within SVZ/VZ is shown. Values are presented as mean ± SD; n = 3 independent experiments. **p < 0.01, one-way ANOVA with Tukey's test for post hoc multiple comparisons.

See also Figures S2–S4.

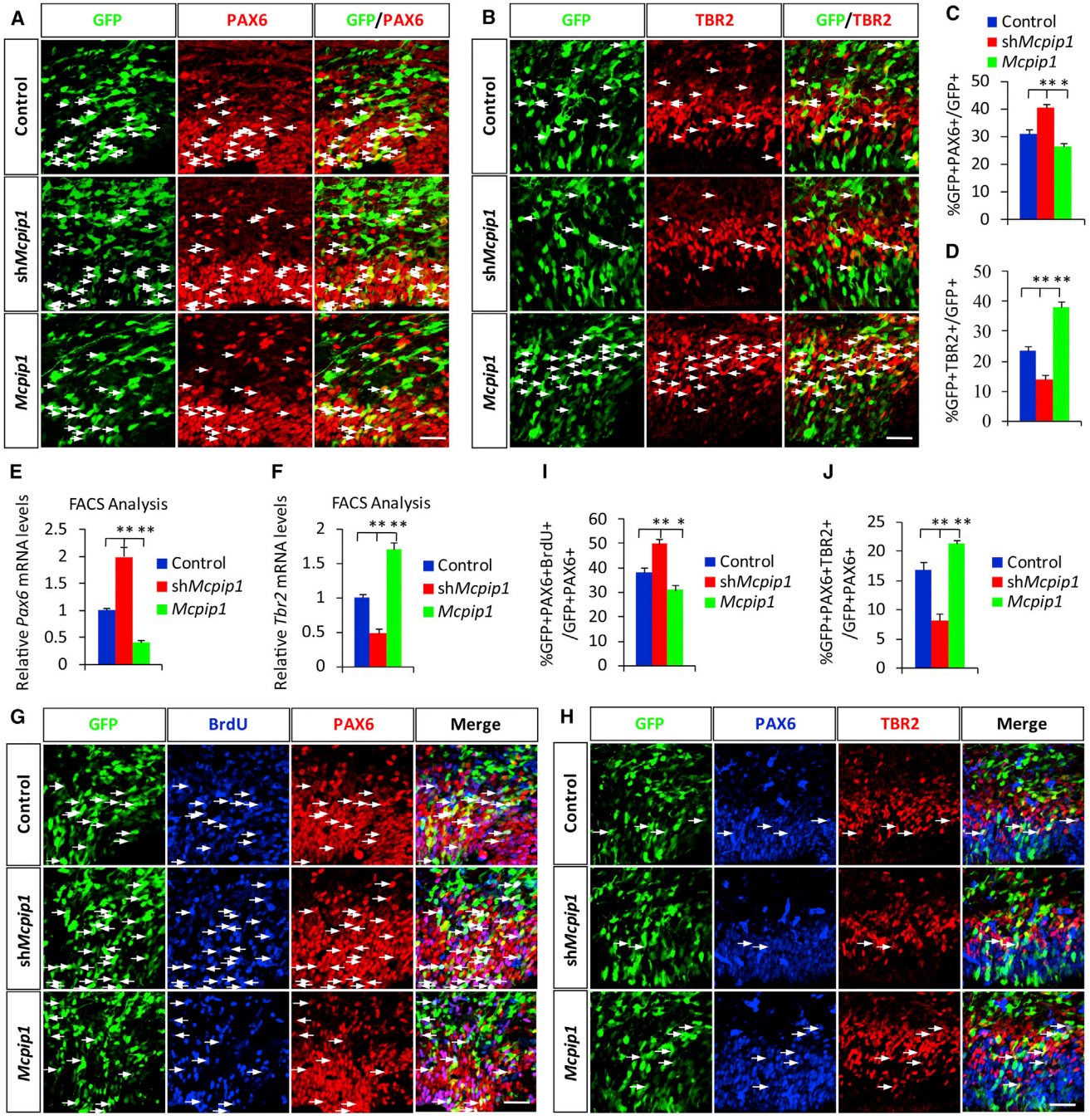

Figure 3. MCPIP1 Regulates the Composition of the NPC Pool and Transition of NPCs

(A–F) MCPIP1 regulates the makeup of the NPC pool. The electroporated E16 brain sections were immunostained with anti-PAX6 or anti-TBR2 antibody. Confocal images of the immunostained brain section (A and B; scale bars, 20 μm) and the quantification results within SVZ/VZ (C–F) are shown. MCPIP1 was overexpressed or knocked down in E12 mouse primary NPCs, and cells were harvested for FACS and qRT-PCR analysis to examine *Pax6* and *Tbr2* mRNA levels after culture for 3 days. Arrows indicate GFP^+ $PAX6^+$ or GFP^+ $TBR2^+$ cells. Values are presented as mean ± SD; n = 3 independent experiments. *p < 0.05, **p < 0.01, one-way ANOVA with Tukey's test for post hoc multiple comparisons.

(legend continued on next page)

maintain the NPC pool and generate a second, transient neural progenitor population of basal progenitors, which are exclusively neurogenic and have limited self-renewal capacity. We speculated that the increased number of apical progenitors was due to enhanced apical progenitor generation, and the reduction in the number of basal progenitors may be caused by an abnormal transition from apical progenitors to basal progenitors. We explored this possibility by electroporating E13 brains with *Mcpip1* shRNA or *Mcpip1* expression plasmid followed by BrdU injection 2 hr before being euthanized at E16. The electroporated brains were stained with PAX6, BrdU, and TBR2 antibodies. The results showed that MCPIP1-inhibited brains exhibited markedly increased the proportion of PAX6-BrdU double-positive apical progenitors and reduced the proportion of PAX6-TBR2 double-positive progenitors, whereas *Mcpip1*-overexpressing brains displayed the opposite proportions (Figures 3G–3J). Taken together, these findings strongly suggest that MCPIP1 inhibits apical progenitor production and enhances basal progenitor transition.

MCPIP1 Binds *Tet* Transcripts Analyzed by PAR-CLIP

Next, we investigated the molecular mechanism by which MCPIP1 regulates neurogenesis during early cortical development. MCPIP1 is a recently identified immune regulator harboring a CCCH-type zinc-finger domain (Liang et al., 2008; Xu et al., 2012). Most of the characterized CCCH-type zinc-finger proteins bind to RNA and regulate mRNA processing, including mRNA maturation, export, modification, and turnover (Brown, 2005; Hall, 2005). We hypothesized that MCPIP1 as an immune regulator may also regulate neurogenesis by regulating processing of RNAs. To identify the targets of MCPIP1, we performed a photoactivatable-ribonucleoside-enhanced crosslinking and immunoprecipitation (PAR-CLIP) assay (Zhao et al., 2014) in mouse neural N2a cells (Figure 4A). In brief, the experiment was performed by overexpression of FLAG-tagged *Mcpip1* in N2a cells. Two days after transfection, 4-thiouridine (4-SU), a photoreactive ribonucleoside analog, was added to the medium. After 16 hr of incubation, cells were collected after UV crosslinking and subjected to immunoprecipitation with anti-FLAG M2 magnetic beads. Immunoblotting was performed to detect the expression (Figure 4B) and immunoprecipitation efficiency of FLAG-*Mcpip1* (Figure 4C). The RNA fragments bound by MCPIP1 were labeled and detected using a biotin labeling kit (Figure 4C). Next, the target protein-RNA complexes were cut out and subsequently treated to separate RNAs. RNAs were sent for cDNA library construction and deep sequence. After basic analysis, the resulting sequence reads were mapped to the mouse genome (mm10), and analyzed using the PARalyzer software. We identified 9,999 MCPIP1 binding sites located in gene regions. Among them, 3,620 sites (36.2%) bound to MCPIP1 via their intronic regions, 2,981 sites (29.8%) bound to MCPIP1 via 3′ UTR, and 1,427 sites (14.3%) were in coding sequence (CDS) (Figure 4D and Table S1). We then used the DREME algorithm (Bailey, 2011) to analyze all utilized sequence reads of binding sites and define the sequence logo of the MCPIP1 recognition motif (Figure 4E).

The molecular basis of DNA demethylation during mammalian development has been prompted by the recent discovery and characterization of the TET family of dioxygenases (Tahiliani et al., 2009). Although some essential roles of TET enzymes in brain development have been reported (Hahn et al., 2013; Lv et al., 2014b; Zhang et al., 2013), the function of TET proteins and their regulation are still poorly elucidated. Based on these previous studies, we focused our work on the TET family among the MCPIP1-binding RNAs. From PAR-CLIP results, we found that both *Tet2* and *Tet3* were included in MCPIP1-binding RNAs, and their binding sites were located in the coding sequence (Table S1). We analyzed all the binding genes, and *Tet2* and *Tet3* had higher mode scores among these genes (Figure 4F). In particular, *Tet3* has two binding sites for MCPIP1 (Figure 4G). These results demonstrate that MCPIP1 directly binds to *Tet2* and *Tet3* and that their interaction is strong. Collectively, these data suggest that the TET family is one of the major targets for MCPIP1. To confirm the direct binding of MCPIP1 to *Tet2* and *Tet3* mRNAs, we performed in vitro experiments with electromobility shift assay (EMSA). The results showed that MCPIP1 protein bound directly to *Tet2* and *Tet3* mRNA (Figure S5A). However, the interaction between MCPIP1 and *Tet2* is not as strong as the interaction between MCPIP1 and *Tet3*. These results are consistent with those in PAR-CLIP experiments, which show that *Tet3* has two binding sites for MCPIP1.

Considering that the mammalian TET family contains three members (TET1, TET2, and TET3) and the PAR-CLIP results, we wondered whether *Tet1* was also an MCPIP1-binding RNA but not detected. Therefore, we further examined the endogenous expression of *Tet1*, *Tet2*, and *Tet3* in N2a cells using absolute qRT-PCR. The results showed

(G–J) MCPIP1 regulates the generation and transition of apical progenitors. (G and H) Embryonic brains were electroporated at E13 and collected at E16. BrdU (100 mg/kg) was injected into mice 2 hr before being euthanized. The electroporated brains were immunostained with anti-PAX6 and anti-BrdU or anti-TBR2 antibody. Arrows indicate GFP^+ $Pax6^+$ $BrdU^+$ or GFP^+ $PAX6^+$ $TBR2^+$ cells. Scale bars, 20 μm. (I and J) Quantification of results within SVZ/VZ. Values are mean ± SD; n = 3 independent experiments. *p < 0.05, **p < 0.01, one-way ANOVA with Tukey's test for post hoc multiple comparisons.

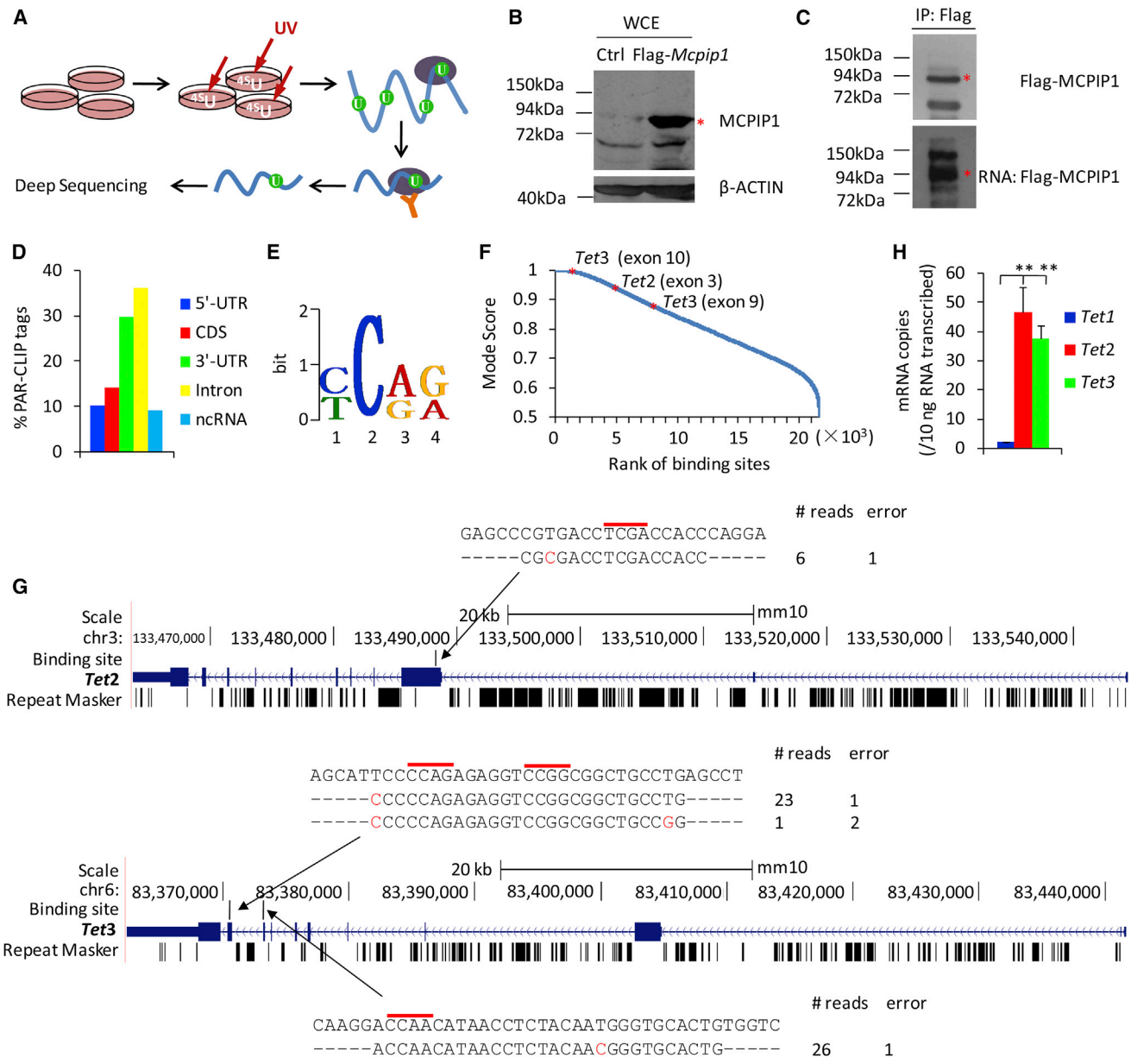

Figure 4. MCPIP1 Binds *Tet* Transcripts Analyzed by PAR-CLIP

(A) Illustration of PAR-CLIP analysis. N2a cells were transfected with FLAG or FLAG-*Mcpip1* plasmids. After culture for 2 days, 200 μM 4-SU was supplemented to the culture medium for 16 hr, and cells were irradiated with 0.4 J/cm^2, 365 nm UV light. After a series of subsequent treatments, MCPIP1-binding RNAs were separated and deep sequenced.

(B) Immunoblot analysis of N2a cells transfected with FLAG or Flag-*Mcpip1* plasmids. The expression levels of MCPIP1 protein in whole-cell extract (WCE) was detected by western blotting with FLAG antibody. Asterisk indicates the position of MCPIP1 protein. Ctrl, FLAG empty vector. β-Actin was used as loading control.

(C) Immunoprecipitation efficiency of MCPIP1 and biotin-labeled MCPIP1 protein-RNA complex. MCPIP1 protein-RNA complex was pulled down with FLAG M2 magnetic beads, and then RNA was labeled and detected according to instructions of biotin labeling kit. Asterisk indicates the FLAG-MCPIP1-RNA complex.

(D) Percentage of MCPIP1 PAR-CLIP tags in mature mRNAs (5′ UTR, CDS, and 3′ UTR), Introns, and non-coding RNAs.

(E) Sequence logo of the MCPIP1 recognition motif generated by DREME analysis of all utilized sequence reads of binding sites.

(F) The ranks of *Tet2* and *Tet3* binding sites on ModeScore among all MCPIP1 binding sites. Asterisk indicates the ModeScore of *Tet2* and *Tet3* binding sites.

(legend continued on next page)

that *Tet1* mRNA levels were significantly lower than *Tet2* and *Tet3* mRNA levels (Figure 4H), which is similar to the results in mouse embryonic neocortex (Hahn et al., 2013). Low *Tet1* expression levels provide a possible explanation for the reason that *Tet1* was not detected in PAR-CLIP experiments. Therefore, in the following experiments we analyzed the regulation of MCPIP1 on TET2 and TET3, as well as TET1.

MCPIP1 Regulates *Tet* mRNA and 5hmC Levels

The potential roles of TET proteins in the immune system have been implied (Suarez-Alvarez et al., 2012; Tsagaratou and Rao, 2013). Combined with the PAR-CLIP results, we originally hypothesized that MCPIP1 as an immune regulator may also regulate the expression of *Tet* genes. To determine the regulation of MCPIP1 on TETs, we performed in vitro NPC culture experiments. Primary NPCs were infected with lentivirus to knock down or overexpress *Mcpip1* and cultured under differentiation conditions. Cells were harvested 3 days later for FACS and qRT-PCR analysis. Consistent with our prediction, *Tet* mRNA levels were increased by *Mcpip1* inhibition, whereas *Tet* mRNA levels were decreased by *Mcpip1* overexpression (Figures 5A and S5B). Further western blot results confirmed that TET protein levels were decreased by *Mcpip1* overexpression (Figures S5C–S5H). These results demonstrate that MCPIP1 regulates the expression of TETs. Due to the ability of TET proteins to convert 5mC to 5hmC (Ito et al., 2010; Tahiliani et al., 2009), we investigated whether MCPIP1 affected 5hmC levels by dot-blot and immunostaining analysis. In the dot-blot experiment, NPCs were infected with *Mcpip1* shRNA or *Mcpip1* expression lentivirus and cultured in differentiation medium for 3 days, and the cells harvested for dot-blot analysis. Consistent with the effects of MCPIP1 on the expression of TETs, *Mcpip1* inhibition markedly enhanced the levels of 5hmC, whereas *Mcpip1* overexpression reduced the levels of 5hmC (Figures 5B, 5C, S5I, and S5J). However, global 5mC levels showed no obvious changes following *Mcpip1* expression variation (Figures 5B, 5C, S5I, and S5J), consistent with previous reports (Fu et al., 2013; Lv et al., 2014b). This is not difficult to understand, considering that the level of 5hmC in cortical DNA only accounts for about 1% of all cytosines or 20%–25% of total 5mC (Jin et al., 2011), so the change of 5hmC would not dramatically affect the global 5mC levels. Our study established a correlation between the expression levels of MCPIP1 and TETs, as well as 5hmC. Collectively, these data demonstrate that MCPIP1 can regulate TET expression and 5hmC levels.

Based on these results, we performed the following experiments to confirm the regulation of MCPIP1 on *Tet* mRNA. Mouse N2a cells were transfected with *Mcpip1* overexpression or vector plasmids, and actinomycin D was added to stop transcription after 48 hr. The cells were harvested to examine the residual level of *Tet* mRNA at different time points. The results showed that MCPIP1 caused a faster decay rate of *Tet* mRNA (Figure 5D). These results indicate that MCPIP1 is directly involved in the regulation of *Tet* mRNA levels.

Our PAR-CLIP analysis showed that MCPIP1 binds to *Tet* mRNA via the coding sequence. To confirm whether MCPIP1 regulates *Tet* mRNA levels through the coding sequence, we constructed *Tet* expression plasmids containing coding sequence but without 3′ UTRs. MCPIP1 contains a PilT N-terminal (PIN) domain, which is responsible for its enzymatic activity (Matsushita et al., 2009; Mizgalska et al., 2009). Aspartic acid at position 141, which forms the enzymatic pocket of PIN domain, is critical for RNase activity (Matsushita et al., 2009). To confirm that RNase activity of MCPIP1 is required for its function, we also constructed *Mcpip1* mutant plasmids with a substitution of aspartic acid for asparagine at position 141 (D141N) (Figure S5K). Additionally the CCCH zinc-finger domain of MCPIP1, located within amino acid residues 305–325, is essential for RNA-binding capacity. *Mcpip1*-Δ305–325 (lacking amino acids 305–325) has been used to demonstrate the importance of this CCCH domain in mRNA and pre-microRNA degradation (Lin et al., 2013; Matsushita et al., 2009; Suzuki et al., 2011). To confirm whether the CCCH domain of MCPIP1 bound *Tet* mRNA and was necessary for its RNase activity, we constructed the *Mcpip1*-Δ305–325 mutant plasmid (Figure S5K). *Tet* expression plasmid was cotransfected with vector plasmid, wild-type *Mcpip1*, *Mcpip1*-D141N, or *Mcpip1*-Δ305–325 plasmid into human embryonic kidney cells (HEK 293T). The qRT-PCR analysis was performed after culture for 3 days, and the results showed that wild-type *Mcpip1* obviously reduced the expression levels of *Tet* mRNA, whereas the point mutation of D141N or the *Mcpip1*-Δ305–325 mutant significantly abolished this effect of *Mcpip1* (Figure 5E). These

(G) Sequence alignments of MCPIP1 PAR-CLIP cDNA sequence reads to the corresponding regions of *Tet2* and *Tet3* transcripts. The number of sequence reads (# reads) and mismatches (errors) are indicated. Red bars indicate the 4-nt MCPIP1 recognition sequence and nucleotides marked in red indicate T-to-C or T-to-G mutations.

(H) Absolute copy numbers of *Tet1*, *Tet2*, and *Tet3* mRNA transcripts in N2a cells were detected by absolute qRT-PCR. N2a cells were collected to extract total RNAs, and qRT-PCR analysis was performed using *Tet1*, *Tet2*, and *Tet3* primers, respectively. Values are mean ± SD; n = 3 independent experiments. **p < 0.01, one-way ANOVA with Tukey's test for post hoc multiple comparisons.

See also Figure S5 and Table S1.

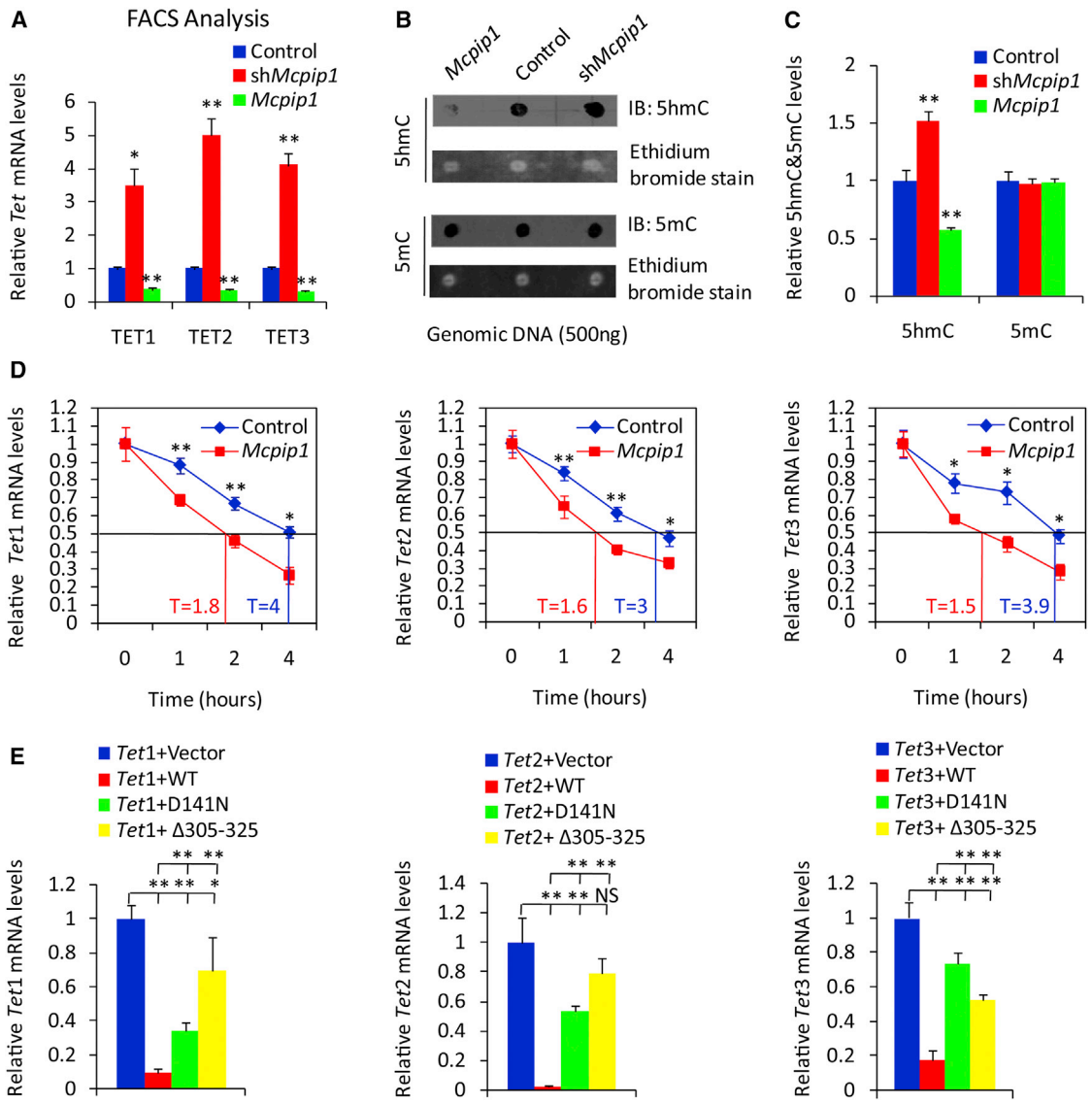

Figure 5. MCPIP1 Regulates *Tet* mRNA Expression and 5hmC Levels

(A) MCPIP1 regulates *Tet* mRNA levels. Mouse NPCs isolated from E12 embryonic brains were infected with *Mcpip1* knockdown or overexpression lentivirus, and collected for FACS and qRT-PCR analysis after culture in differentiation medium for 3 days. Relative *Tet* mRNA levels were normalized to the expression of *β-Actin*. Values are mean ± SD; n = 3 independent experiments. *p < 0.05, **p < 0.01, one-way ANOVA with Tukey's test for post hoc multiple comparisons.

(B and C) Dot blot (B) shows that the relative 5hmC not 5mC levels significantly change after *Mcpip1* expression alteration. Mouse NPCs isolated from E12 embryonic brains were infected with *Mcpip1* knockdown or overexpression lentivirus, and collected for DNA extraction after culture for 3 days in differentiation medium. DNA (500 ng) for each sample was used for dot-blot analysis with anti-5hmC or anti-5mC antibody. Graphs (C) show the quantification results. Values are mean ± SD; n = 3 independent experiments. **p < 0.01, one-way ANOVA with Tukey's test for post hoc multiple comparisons.

(D) Effects of MCPIP1 on the decay rate of *Tet* mRNA. *Mcpip1* or vector plasmids were transfected into N2a cells. Actinomycin D (5 μg/mL) was added to stop transcription after 48 hr. The cells were harvested for RNA extraction at the indicated times, and the *Tet* mRNA levels were determined by qRT-PCR and normalized by *β-Actin*. The quantification shows the relative *Tet* mRNA at each time point, compared with the level of *Tet* mRNA at time zero, taken as 1. Meanwhile, the half-life of *Tet* mRNA is calculated and shown as T value. Values are mean ± SD; n = 3 independent experiments. *p < 0.05, **p < 0.01, two-tailed Student's t test.

(E) The RNase activity of MCPIP1 and the CCCH zinc-finger domain of MCPIP1 are required for the regulation of *Tets*. *Tet* (*Tet1*, *Tet2*, or *Tet3*) plasmids were cotransfected with *Mcpip1* (WT), *Mcpip1*-D141N mutant, the *Mcpip1*-Δ305–325 mutant or vector plasmids into HEK293T

(legend continued on next page)

results suggest that MCPIP1 regulates *Tet* mRNA levels by its RNase activity and that the CCCH domain of MCPIP1 is essential for its RNase activity. However, our results showed that MCPIP1 could regulate *Tet* mRNA by targeting its coding sequence but not 3′ UTR as inflammation-related mRNAs as in previous reports (Lin et al., 2013; Matsushita et al., 2009; Uehata et al., 2013). Taken together, these results suggest diversity of MCPIP1 action mode in regulating gene expression as an RNA-binding protein with RNase activity.

To demonstrate how TETs or DNA demethylations affect early cortical neurogenesis, we constructed *Tet* knockdown plasmids that efficiently silenced *Tet* expression (Figures S6A–S6C), and tested the expression change of several important genes required for early cortical neurogenesis after *Tet* expression was reduced. Primary NPCs infected with *Tet* (*Tet1*, *Tet2*, or *Tet3*) knockdown lentivirus were collected for FACS and qRT-PCR analysis after culturing in differentiation medium for 3 days. The results showed that *Tet* knockdown resulted in markedly decreased expression of the transcription factor SRY (sex-determining region) box 2 (*Sox2*), yes-associated protein 1 (*Yap1*), and RE1-silencing transcription factor (*REST*) in cortical NPCs under differentiation conditions, whereas *β-Catenin* expression was only significantly affected by *Tet1* knockdown, and *Cyclin D1* showed no significant change after *Tet* expression inhibition (Figure S5L). These results demonstrated that TETs affect early cortical neurogenesis by regulating downstream genes required for neurogenesis.

MCPIP1/TETs Functionally Regulate Neurogenesis and Maintain the NPC Pool

Our findings raised the possibility that MCPIP1 interaction with TETs may be involved in co-regulation of early cortical neurogenesis and maintenance of the NPC pool. To further examine the relationship between MCPIP1 and TETs during early neocortical development, we determined whether silencing *Tet* expression could rescue the in vivo cellular phenotypes due to reduced *Mcpip1* expression. In utero electroporation was performed at E13, followed by BrdU injection 2 hr before euthanasia at E16. Notably, we observed that the cell distribution change caused by *Mcpip1* knockdown in the cortex was completely rescued by TETs (Figures 6A and 6B). Co-expression of *Tet* shRNA with *Mcpip1* shRNA completely rescued the defects of neurogenesis caused by *Mcpip1* knockdown. We observed that *Tet* knockdown led to a significant increase in MAP2-positive (Figures 6C and 6D) and TUJ1-positive cells (Figures S6D and S6E), as well as an obvious reduction in BrdU and pH3 incorporation (Figures S6F–S6I) compared with *Mcpip1* knockdown. Meanwhile, the unbalanced proportion of apical and basal progenitors in the NPC pool caused by *Mcpip1* knockdown was reversed (Figures 6F–6I). To further confirm these results, we performed in vitro FACS and qRT-PCR analysis and obtained consistent results (Figures 6J and 6K). In addition, the increased 5hmC level caused by *Mcpip1* knockdown could be rescued by knockdown of *Tets*, which demonstrate TETs as mediators of the effects on 5hmC levels (Figures S6J and S6K). Collectively, these data strongly supported the functions of MCPIP1 in regulating early cortical neurogenesis and maintenance of the NPC pool through mediating *Tet* expression.

DISCUSSION

Although the brain has traditionally been regarded as immune-privileged, many studies suggest that there is extensive communication between the immune system and the nervous system in both healthy and diseased conditions. We sought here to learn about the basic roles of specific and crucial immune molecules in the nervous system. We observed that MCPIP1 was abundant in early neural progenitors and that its expression decreased over time during early mouse neocortical development. In the murine cortex, neurogenesis begins at approximately E12, reaches a peak at approximately E15, and terminates at approximately E18 (Qian et al., 2000). Therefore, MCPIP1 expression in the developing neocortex suggested precise temporal and spatial roles for MCPIP1 during this period. We identified these roles by demonstrating that altered *Mcpip1* expression resulted in changes of various aspects of neurogenesis. Notably, the composition of the neural progenitor pool was altered following *Mcpip1* expression variation, resulting in a change in the relative proportion of apical progenitors to basal progenitors. A potentially interesting possibility was explored, showing that MCPIP1 inhibited apical progenitor generation but promoted its transition.

Next, we investigated the underlying mechanism for MCPIP1 in early cortical neurogenesis. It is known that active DNA demethylation is prevalent in mammals (Tan and Shi, 2012). TET proteins were recently identified as enzymes that promote DNA demethylation (Ito et al., 2010; Tahiliani et al., 2009). Direct regulation of *Tet* expression

cells, and cells were collected 3 days later. The relative *Tet1*, *Tet2*, or *Tet3* levels were determined by qRT-PCR and normalized by *β-Actin*. Values are mean ± SD; n = 3 independent experiments. *p < 0.05, **p < 0.01, one-way ANOVA with Tukey's test for post hoc multiple comparisons; NS, not significant.
See also Figure S5.

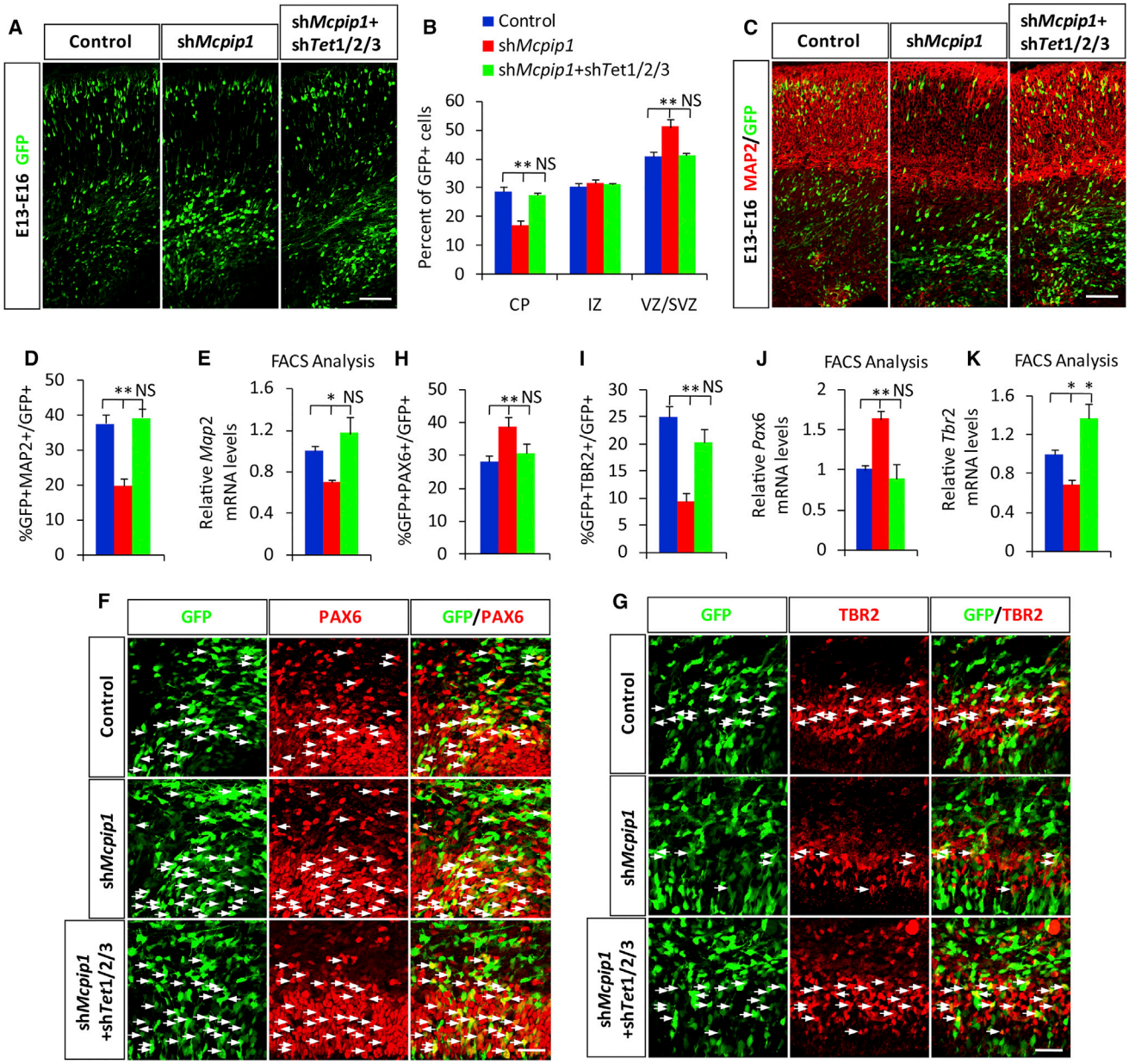

Figure 6. MCPIP1/TETs Functionally Regulate Neurogenesis and Maintain the NPC Pool

(A and B) The changed cell distribution caused by *Mcpip1* inhibition is rescued by *Tet* knockdown (sh*Tet1*, sh*Tet2*, and sh*Tet3*). (A) Embryonic brains were electroporated at E13 and collected at E16. Scale bar, 50 μm. (B) The percentage of GFP cells in each zone was quantified. Values are presented as mean ± SD; n = 3 independent experiments. **p < 0.01, one-way ANOVA with Tukey's test for post hoc multiple comparisons; NS, not significant.

(C–E) Decreased MAP2-positive cells caused by *Mcpip1* knockdown is rescued by *Tet* knockdown. (C) The electroporated E16 brain section was immunostained with anti-MAP2 antibody. Scale bar, 50 μm. Graph (D) shows the quantification of MAP2-GFP double-positive cells. *Map2* mRNA level downregulation caused by *Mcpip1* knockdown in E12 mouse primary NPCs is rescued by *Tet* knockdown, determined by FACS and qRT-PCR analysis (E). Values are presented as mean ± SD; n = 3 independent experiments. *p < 0.05, **p < 0.01, one-way ANOVA with Tukey's test for post hoc multiple comparisons; NS, not significant.

(F–K) The unbalanced number of apical progenitor and basal progenitor in the NPC pool is rescued by TETs. The electroporated E16 brain sections were immunostained with anti-PAX6 (F) or anti-TBR2 antibody (G). Arrows indicate GFP$^+$ PAX6$^+$ or GFP$^+$ TBR2$^+$ cells. Scale bars, 20 μm. The percentage of PAX6-GFP (H) or TBR2-GFP (I) double-positive cells within SVZ/VZ is quantified. (J and K) *Pax6* and *Tbr2* mRNA

(legend continued on next page)

should be a rather straightforward means of modulating the level of DNA modification. Although regulation of *Tet* expression at the transcriptional level is well documented (Fu et al., 2013; Song et al., 2013), insights into the direct regulation of *Tet* mRNA by an RNA-binding protein are reported herein.

Recent studies have demonstrated that the post-transcriptional control of gene expression at the mRNA level is as important as transcriptional control (Anderson, 2008; Hao and Baltimore, 2009). MCPIP1 is an RNase and is responsible for degrading a set of inflammatory transcripts as well as pre-microRNAs (Matsushita et al., 2009; Mizgalska et al., 2009; Suzuki et al., 2011). PAR-CLIP analysis has been extensively used in target identification for RNA-binding proteins (Hafner et al., 2010; Yoon et al., 2014). Therefore, we performed PAR-CLIP analysis to identify genes bound by MCPIP1 in mouse neural N2a cells, but not human HEK293 cells, which have been widely used in CLIP analysis. This is because the N2a cell is a mouse neural cell, which more closely resembles mouse NPCs than human HEK293 cells. However, the mouse genome is less annotated, and the results from two cell lines may be different. A large number of genes binding to MCPIP1 were identified by PAR-CLIP analysis. Among them, we found that *Tets* have a strong interaction with MCPIP1. Low levels of *Tet1* expression may provide an explanation for its non-detection. An in vitro EMSA experiment further confirmed the direct interaction between MCPIP1 protein and *Tet* mRNA. These results indicate that TETs are one of the major targets for MCPIP1.

There are many post-transcriptional regulation modes of RNA-binding proteins for their target genes. Binding sites located in coding sequence contribute most to translational repression while binding sites located in 3′ UTR mainly affect transcript stabilization (Brummer et al., 2013). Our findings showed that MCPIP1 bound to the coding sequence of *Tets* and regulated *Tet* mRNA levels. Further studies showed that its RNase activity was necessary for MCPIP1 regulation on *Tet* mRNA. However, the mechanism of MCPIP1 regulation on *Tet* mRNA by its coding sequence needs further work. Our current findings indicate the diversity of MCPIP1 action mode in regulating gene expression as an RNA-binding protein with RNase activity. These results will be essential to further our understanding of direct regulation of *Tet* expression.

In summary, this study clearly demonstrated an essential contribution for MCPIP1 in early neocortical development, which provides a basis for understanding the functions of MCPIP1 in the developing brain. Thus, these results suggested that MCPIP1 may be a potential therapeutic target for the treatment of neural developmental disorders by direct manipulation of immune or non-immune signaling within the brain.

EXPERIMENTAL PROCEDURES

Animals

Pregnant ICR mice were purchased from Vital River Laboratories. All animal studies were performed in accordance with experimental protocols and approved by Animal Care and Use Committees at the Institute of Zoology, Chinese Academy of Sciences.

Photoactivatable Ribonucleoside-Enhanced Crosslinking and Immunoprecipitation Analysis

The PAR-CLIP analysis was carried out as in previous work (Zhao et al., 2014), and performed in N2a cells by overexpression of FLAG-tagged *Mcpip1*. Detailed information of PAR-CLIP can be found in Supplemental Experimental Procedures.

In Utero Electroporation

In utero electroporation was performed as in previous work (Lv et al., 2014a), and described in detail in Supplemental Experimental Procedures.

Statistical Analysis

Statistical analyses, including two-tailed Student's t tests and one-way ANOVA followed by a Tukey's test for post hoc multiple comparisons, were performed using SPSS 16.0 for Windows. Differences were considered statistically significant at $*p < 0.05$ and $**p < 0.01$. Data are presented as mean ± SD.

Additional methods are provided in Supplemental Experimental Procedures.

SUPPLEMENTAL INFORMATION

Supplemental Information includes Supplemental Experimental Procedures, six figures, and one table and can be found with this article online at http://dx.doi.org/10.1016/j.stemcr.2016.07.011.

AUTHOR CONTRIBUTIONS

H.J. and X.L. designed parts of the study, performed the research, analyzed the data, and wrote the manuscript; X.L., Y.Y., and X.Y. performed the research; J.J. designed parts of the study, supported the finance, and approved the final manuscript.

level variation caused by *Mcpip1* knockdown could be rescued by *Tet* knockdown, determined by FACS and qRT-PCR analysis. Values are mean ± SD; n = 3 independent experiments. $*p < 0.05$, $**p < 0.01$, one-way ANOVA with Tukey's test for post hoc multiple comparisons; NS, not significant.
See also Figure S6.

ACKNOWLEDGMENTS

We thank Dr. Wei Shao for his critical comments. We thank Susan Lin for revising the English language. This work was supported by grants from the Ministry of Science and Technology of China (2014CB964903 and 2015CB964500 J.J.), the National Science Foundation of China (31371477), the Strategic Priority Research Program (XDA01020301), and China Postdoctoral Science Foundation Fellowships (X.L. and H.J.).

Received: November 28, 2015
Revised: July 10, 2016
Accepted: July 11, 2016
Published: August 11, 2016

REFERENCES

Anderson, P. (2008). Post-transcriptional control of cytokine production. Nat. Immunol. *9*, 353–359.

Bailey, T.L. (2011). DREME: motif discovery in transcription factor ChIP-seq data. Bioinformatics *27*, 1653–1659.

Bauer, S., Kerr, B.J., and Patterson, P.H. (2007). The neuropoietic cytokine family in development, plasticity, disease and injury. Nat. Rev. Neurosci. *8*, 221–232.

Boulanger, L.M. (2009). Immune proteins in brain development and synaptic plasticity. Neuron *64*, 93–109.

Brown, R.S. (2005). Zinc finger proteins: getting a grip on RNA. Curr. Opin. Struct. Biol. *15*, 94–98.

Brummer, A., Kishore, S., Subasic, D., Hengartner, M., and Zavolan, M. (2013). Modeling the binding specificity of the RNA-binding protein GLD-1 suggests a function of coding region-located sites in translational repression. RNA *19*, 1317–1326.

Carpentier, P.A., and Palmer, T.D. (2009). Immune influence on adult neural stem cell regulation and function. Neuron *64*, 79–92.

Fu, X., Jin, L., Wang, X., Luo, A., Hu, J., Zheng, X., Tsark, W.M., Riggs, A.D., Ku, H.T., and Huang, W. (2013). MicroRNA-26a targets ten eleven translocation enzymes and is regulated during pancreatic cell differentiation. Proc. Natl. Acad. Sci. USA *110*, 17892–17897.

Guo, J.U., Ma, D.K., Mo, H., Ball, M.P., Jang, M.H., Bonaguidi, M.A., Balazer, J.A., Eaves, H.L., Xie, B., Ford, E., et al. (2011a). Neuronal activity modifies the DNA methylation landscape in the adult brain. Nat. Neurosci. *14*, 1345–1351.

Guo, J.U., Su, Y., Zhong, C., Ming, G.L., and Song, H. (2011b). Hydroxylation of 5-methylcytosine by TET1 promotes active DNA demethylation in the adult brain. Cell *145*, 423–434.

Hafner, M., Landthaler, M., Burger, L., Khorshid, M., Hausser, J., Berninger, P., Rothballer, A., Ascano, M., Jr., Jungkamp, A.C., Munschauer, M., et al. (2010). Transcriptome-wide identification of RNA-binding protein and microRNA target sites by PAR-CLIP. Cell *141*, 129–141.

Hahn, M.A., Qiu, R., Wu, X., Li, A.X., Zhang, H., Wang, J., Jui, J., Jin, S.G., Jiang, Y., Pfeifer, G.P., and Lu, Q. (2013). Dynamics of 5-hydroxymethylcytosine and chromatin marks in mammalian neurogenesis. Cell Rep. *3*, 291–300.

Hall, T.M. (2005). Multiple modes of RNA recognition by zinc finger proteins. Curr. Opin. Struct. Biol. *15*, 367–373.

Hao, S., and Baltimore, D. (2009). The stability of mRNA influences the temporal order of the induction of genes encoding inflammatory molecules. Nat. Immunol. *10*, 281–288.

He, Y.F., Li, B.Z., Li, Z., Liu, P., Wang, Y., Tang, Q., Ding, J., Jia, Y., Chen, Z., Li, L., et al. (2011). Tet-mediated formation of 5-carboxylcytosine and its excision by TDG in mammalian DNA. Science *333*, 1303–1307.

Ito, S., D'Alessio, A.C., Taranova, O.V., Hong, K., Sowers, L.C., and Zhang, Y. (2010). Role of Tet proteins in 5mC to 5hmC conversion, ES-cell self-renewal and inner cell mass specification. Nature *466*, 1129–1133.

Jin, S.G., Jiang, Y., Qiu, R., Rauch, T.A., Wang, Y., Schackert, G., Krex, D., Lu, Q., and Pfeifer, G.P. (2011). 5-Hydroxymethylcytosine is strongly depleted in human cancers but its levels do not correlate with IDH1 mutations. Cancer Res. *71*, 7360–7365.

Komal, P., Gudavicius, G., Nelson, C.J., and Nashmi, R. (2014). T-cell receptor activation decreases excitability of cortical interneurons by inhibiting alpha7 nicotinic receptors. J. Neurosci. *34*, 22–35.

Liang, J., Wang, J., Azfer, A., Song, W., Tromp, G., Kolattukudy, P.E., and Fu, M. (2008). A novel CCCH-zinc finger protein family regulates proinflammatory activation of macrophages. J. Biol. Chem. *283*, 6337–6346.

Liang, J., Saad, Y., Lei, T., Wang, J., Qi, D., Yang, Q., Kolattukudy, P.E., and Fu, M. (2010). MCP-induced protein 1 deubiquitinates TRAF proteins and negatively regulates JNK and NF-kappaB signaling. J. Exp. Med. *207*, 2959–2973.

Lin, R.J., Chien, H.L., Lin, S.Y., Chang, B.L., Yu, H.P., Tang, W.C., and Lin, Y.L. (2013). MCPIP1 ribonuclease exhibits broad-spectrum antiviral effects through viral RNA binding and degradation. Nucleic Acids Res. *41*, 3314–3326.

Lv, X., Jiang, H., Li, B., Liang, Q., Wang, S., Zhao, Q., and Jiao, J. (2014a). The crucial role of Atg5 in cortical neurogenesis during early brain development. Sci. Rep. *4*, 6010.

Lv, X., Jiang, H., Liu, Y., Lei, X., and Jiao, J. (2014b). MicroRNA-15b promotes neurogenesis and inhibits neural progenitor proliferation by directly repressing TET3 during early neocortical development. EMBO Rep. *15*, 1305–1314.

Matsushita, K., Takeuchi, O., Standley, D.M., Kumagai, Y., Kawagoe, T., Miyake, T., Satoh, T., Kato, H., Tsujimura, T., Nakamura, H., et al. (2009). Zc3h12a is an RNase essential for controlling immune responses by regulating mRNA decay. Nature *458*, 1185–1190.

Mizgalska, D., Wegrzyn, P., Murzyn, K., Kasza, A., Koj, A., Jura, J., and Jarzab, B. (2009). Interleukin-1-inducible MCPIP protein has structural and functional properties of RNase and participates in degradation of IL-1beta mRNA. FEBS J. *276*, 7386–7399.

Qian, X., Shen, Q., Goderie, S.K., He, W., Capela, A., Davis, A.A., and Temple, S. (2000). Timing of CNS cell generation: a programmed sequence of neuron and glial cell production from isolated murine cortical stem cells. Neuron *28*, 69–80.

Sallusto, F., Impellizzieri, D., Basso, C., Laroni, A., Uccelli, A., Lanzavecchia, A., and Engelhardt, B. (2012). T-cell trafficking in the central nervous system. Immunol. Rev. *248*, 216–227.

Skalniak, L., Mizgalska, D., Zarebski, A., Wyrzykowska, P., Koj, A., and Jura, J. (2009). Regulatory feedback loop between NF-kappaB and MCP-1-induced protein 1 RNase. FEBS J. *276*, 5892–5905.

Song, S.J., Poliseno, L., Song, M.S., Ala, U., Webster, K., Ng, C., Beringer, G., Brikbak, N.J., Yuan, X., Cantley, L.C., et al. (2013). MicroRNA-antagonism regulates breast cancer stemness and metastasis via TET-family-dependent chromatin remodeling. Cell *154*, 311–324.

Suarez-Alvarez, B., Rodriguez, R.M., Fraga, M.F., and Lopez-Larrea, C. (2012). DNA methylation: a promising landscape for immune system-related diseases. Trends Genet. *28*, 506–514.

Suzuki, H.I., Arase, M., Matsuyama, H., Choi, Y.L., Ueno, T., Mano, H., Sugimoto, K., and Miyazono, K. (2011). MCPIP1 ribonuclease antagonizes dicer and terminates microRNA biogenesis through precursor microRNA degradation. Mol. Cell *44*, 424–436.

Syken, J., and Shatz, C.J. (2003). Expression of T cell receptor beta locus in central nervous system neurons. Proc. Natl. Acad. Sci. USA *100*, 13048–13053.

Tahiliani, M., Koh, K.P., Shen, Y., Pastor, W.A., Bandukwala, H., Brudno, Y., Agarwal, S., Iyer, L.M., Liu, D.R., Aravind, L., and Rao, A. (2009). Conversion of 5-methylcytosine to 5-hydroxymethylcytosine in mammalian DNA by MLL partner TET1. Science *324*, 930–935.

Tan, L., and Shi, Y.G. (2012). Tet family proteins and 5-hydroxymethylcytosine in development and disease. Development *139*, 1895–1902.

Tsagaratou, A., and Rao, A. (2013). TET proteins and 5-methylcytosine oxidation in the immune system. Cold Spring Harb. Symp. Quant. Biol. *78*, 1–10.

Uehata, T., Iwasaki, H., Vandenbon, A., Matsushita, K., Hernandez-Cuellar, E., Kuniyoshi, K., Satoh, T., Mino, T., Suzuki, Y., Standley, D.M., et al. (2013). Malt1-induced cleavage of regnase-1 in CD4(+) helper T cells regulates immune activation. Cell *153*, 1036–1049.

Xu, J., Fu, S., Peng, W., and Rao, Z. (2012). MCP-1-induced protein-1, an immune regulator. Protein Cell *3*, 903–910.

Yoon, J.H., De, S., Srikantan, S., Abdelmohsen, K., Grammatikakis, I., Kim, J., Kim, K.M., Noh, J.H., White, E.J., Martindale, J.L., et al. (2014). PAR-CLIP analysis uncovers AUF1 impact on target RNA fate and genome integrity. Nat. Commun. *5*, 5248.

Zhang, R.R., Cui, Q.Y., Murai, K., Lim, Y.C., Smith, Z.D., Jin, S., Ye, P., Rosa, L., Lee, Y.K., Wu, H.P., et al. (2013). Tet1 regulates adult hippocampal neurogenesis and cognition. Cell Stem Cell *13*, 237–245.

Zhao, X., Yang, Y., Sun, B.F., Shi, Y., Yang, X., Xiao, W., Hao, Y.J., Ping, X.L., Chen, Y.S., Wang, W.J., et al. (2014). FTO-dependent demethylation of N6-methyladenosine regulates mRNA splicing and is required for adipogenesis. Cell Res. *24*, 1403–1419.

Zhou, L., Azfer, A., Niu, J., Graham, S., Choudhury, M., Adamski, F.M., Younce, C., Binkley, P.F., and Kolattukudy, P.E. (2006). Monocyte chemoattractant protein-1 induces a novel transcription factor that causes cardiac myocyte apoptosis and ventricular dysfunction. Circ. Res. *98*, 1177–1185.